Pik3r1 Is Required for Glucocorticoid-Induced Perilipin 1 Phosphorylation in Lipid Droplet for Adipocyte Lipolysis

Taiyi Kuo,[1,2] Tzu-Chieh Chen,[2,3] Rebecca A. Lee,[1,2] Nguyen Huynh Thao Nguyen,[2] Augusta E. Broughton,[2] Danyun Zhang,[2] and Jen-Chywan Wang[1,2,3]

Glucocorticoids promote lipolysis in white adipose tissue (WAT) to adapt to energy demands under stress, whereas superfluous lipolysis causes metabolic disorders, including dyslipidemia and hepatic steatosis. Glucocorticoid-induced lipolysis requires the phosphorylation of cytosolic hormone-sensitive lipase (HSL) and perilipin 1 (Plin1) in the lipid droplet by protein kinase A (PKA). We previously identified Pik3r1 (also called *p85α*) as a glucocorticoid receptor target gene. Here, we found that glucocorticoids increased HSL phosphorylation, but not Plin1 phosphorylation, in adipose tissue-specific *Pik3r1*-null (AKO) mice. Furthermore, in lipid droplets, the phosphorylation of HSL and Plin1 and the levels of catalytic and regulatory subunits of PKA were increased by glucocorticoids in wild-type mice. However, these effects were attenuated in AKO mice. In agreement with reduced WAT lipolysis, glucocorticoid-initiated hepatic steatosis and hypertriglyceridemia were improved in AKO mice. Our data demonstrated a novel role of Pik3r1 that was independent of the regulatory function of phosphoinositide 3-kinase in mediating the metabolic action of glucocorticoids. Thus, the inhibition of Pik3r1 in adipocytes could alleviate lipid disorders caused by excess glucocorticoid exposure.

Endogenous glucocorticoids (GCs) are steroid hormones released from the adrenal glands in response to stress signals. During fasting, GCs promote lipolysis in white adipose tissue (WAT), where triglycerides (TGs) are hydrolyzed to glycerol and fatty acids as energy fuels. Glycerol serves a precursor for hepatic gluconeogenesis, whereas mobilized fatty acids are oxidized in energy-requiring tissues to produce ATP. However, prolonged GC exposure results in dyslipidemia, hepatic steatosis, and insulin resistance (1–3). Although exogenous GCs are frequently prescribed as effective anti-inflammatory agents, their actions in metabolic tissues pose a therapeutic conundrum (4).

GCs relay their message through the intracellular GC receptor (GR), which is a transcription factor. GC-induced adipocyte lipolysis requires de novo protein synthesis (5–7), which is consistent with the concept that the GR exerts its main function through modulating gene expression. Several mechanisms are documented. First, the GCs increase the transcription of genes encoding lipolytic enzymes, including adipose TG lipase (ATGL; also called desnutrin) and hormone-sensitive lipase (HSL) (6,8,9). ATGL catalyzes the hydrolysis of TG to diacylglycerol, whereas HSL hydrolyzes diacylglycerol to monoacylglycerol (10,11). Moreover, GCs elevate the levels of cAMP (12–14), which activates protein kinase A (PKA). PKA phosphorylates HSL in the cytosol and perilipin 1 (Plin1) on the lipid droplet (10,11). Phosphorylated HSL (pHSL) are mobilized to the lipid droplet and associate with phosphorylated Plin1 (pPlin1) (15–17). This anchoring of pHSL to the lipid droplet is critical, since TGs are stored within the lipid droplet. Upon phosphorylation of Plin1, the interaction between Plin1 and CGI-58 is disrupted, which allows the activation of ATGL by CGI-58 (10,18,19). It has been shown that GCs exert at least two distinct mechanisms to elevate cAMP levels in adipocytes. GCs decrease the expression of Akt (20) and cAMP phosphodiesterase 3B (PDE3B) to augment cAMP levels (14). Alternatively, GCs induce the transcription of *angiopoietin-like 4* (*Angptl4*)

---

(21), which encodes a secreted protein that activates cAMP-PKA signaling in adipocytes to stimulate lipolysis (12). Overall, we propose that GCs promote WAT lipolysis through a network of GR primary target genes, including *ATGL, HSL,* and *Angptl4,* most of which remain to be discovered.

We identified *Pik3r1* (also called *p85α*) as a GR primary target gene in both adipocytes and myotubes with RNA profiling and chromatin immunoprecipitation sequencing analysis (8,22). *Pik3r1* encodes a regulatory subunit of phosphoinositide 3-kinase (PI3K), and overexpression of Pik3r1 reduces insulin signaling in myotubes and hepatocytes (22–25). Monomeric Pik3r1 competes with heterodimeric PI3K, which is composed of Pik3r1 and p110 (the catalytic subunit of PI3K), from binding to insulin receptor substrate-1 (26,27). Since Pik3r1 lacks the catalytic capacity, insulin signaling is attenuated. Alternatively, Pik3r1 can potentiate phosphatase and tensin homolog (PTEN) to inhibit PI3K (28,29). These data illustrate that an increase in Pik3r1 is negatively associated with insulin sensitivity.

In adipocytes, insulin suppresses lipolysis partly through the PI3K-Atk-PDE3B pathway to decrease the levels of cAMP (30–32). Therefore, GC-induced excess Pik3r1 could attenuate insulin signaling and in turn promote lipolysis. To investigate the role of Pik3r1 in lipolysis, we generated adipose tissue–specific Pik3r1 knockout (AKO) mice. Surprisingly, lack of Pik3r1 did not attenuate the PI3K-Atk-PDE3B pathway. Instead, we found that the levels of pPlin1 were significantly decreased in inguinal WAT (iWAT) and epididymal WAT (eWAT) in AKO mice in response to GCs. Furthermore, in lipid droplets of wild-type (WT) mice, subunits of PKA were increased by GC treatment. However, this action was abolished in AKO mice. Moreover, pHSL levels in lipid droplets were augmented by dexamethasone (Dex) in WT mice, and this effect was not seen in AKO mice. Finally, Dex-induced hepatic steatosis and hypertriglyceridemia were dramatically improved in AKO mice. In summary, we have shown that Pik3r1 mediates the metabolic actions of GCs in WAT. Our data underscore the possibility that antagonists of WAT Pik3r1 may improve the adverse effects of GC therapeutics.

RESEARCH DESIGN AND METHODS

Mice
Mice with a conditional allele of the Pik3r1 gene flanked with LoxP sites at exon7 (*Pik3r1^{flox/flox}*) were provided by the laboratory of Lewis Cantley (Weill Cornell Medical College, New York, NY) (33). Mice expressing Cre recombinase driven by the adiponectin promoter (AdipoQ-*Cre*) (34) were purchased from The Jackson Laboratory. AKO mice were generated by crossing *Pik3r1^{flox/flox}* with AdipoQ-*Cre* mice. Primer sequences used for genotyping are listed in Supplementary Table 1. The Office of Laboratory Animal Care at the University of California, Berkeley (AUP-2014–08–6617) approved all animal experiments conducted.

Free Fatty Acid Measurement
Plasma free fatty acid (FFA) levels were measured by a FFA quantification kit (MAK044; Sigma-Aldrich, St. Louis, MO).

Ex Vivo Lipolysis Assay
Lipolysis was assessed as previously described (12). Explants from freshly removed eWAT and iWAT depots (~100 mg) were incubated at 37°C in 500 μL of Krebs-Ringer buffer (12 mmol/L HEPES, 121 mmol/L NaCl, 4.9 mmol/L KCl, 1.2 mmol/L MgSO$_4$, and 0.33 mmol/L CaCl$_2$) with 3% BSA and 3 mmol/L glucose. Media were collected after 1 h of incubation, and glycerol levels in media were determined with free glycerol reagent (F6428; Sigma-Aldrich). Measurements were normalized to protein content of the explants with a protein dye reagent (500–0006; Bio-Rad, Hercules, CA).

Quantitative Real-Time PCR
Quantitative real-time PCR was performed as previously described (35). Primer sequences are listed in Supplementary Table 1.

Isolation of Lipid Droplets
The isolation of lipid droplets was based on a previous report (36). Freshly removed WAT depots were incubated at 37°C in Krebs-Ringer buffer (12 mmol/L HEPES, 121 mmol/L NaCl, 4.9 mmol/L KCl, 1.2 mmol/L MgSO$_4$, and 0.33 mmol/L CaCl$_2$) with 3% BSA, 3 mmol/L glucose, and collagenase (0.033 g/100 mL). The adipocyte solution was washed twice with PBS to remove extra collagenase, followed by resuspension in 3 mL of disruption buffer (25 mmol/L Tris-HCl, 100 mmol/L KCl, 1 mmol/L EDTA, 5 mmol/L EGTA, and protease inhibitor). Cells were disrupted with a Dounce homogenizer, and the lysate was collected and mixed with an equal volume of disruption buffer containing 1.08 mol/L sucrose. It was then sequentially overlaid with 2 mL of 270 mmol/L sucrose buffer, 135 mmol/L sucrose buffer, and Tris/EDTA/EGTA buffer (25 mmol/L Tris-HCl, 1 mmol/L EDTA, 1 mmol/L EGTA, pH 7.4). After centrifugation at 150,000g for 1 h, lipid droplet–enriched fractions were collected from the top of the gradient and were subjected to immunoblotting.

Plasma Insulin Measurement
Plasma insulin levels were measured using an ultrasensitive mouse insulin ELISA kit (Crystal Chem Inc., Downers Grove, IL).

Western Blot and Antibodies
The following antibodies were used in this study: anti-GAPDH (sc-25778; Santa Cruz Biotechnology, Dallas, TX); anti-Pik3r1 (4292s; Cell Signaling Technology, Danvers, MA), anti-ATGL (2138s; Cell Signaling Technology); anti-Akt (9272s; Cell Signaling Technology); anti–phospho-Akt (T308) (9275s; Cell Signaling Technology); anti–perilipin A (ab3526; Abcam, Cambridge, MA); anti–phospho-perilipin (4856; VALA Sciences, San Diego, CA); anti-HSL (4107s; Cell Signaling Technology); anti–phospho-HSL (S660) (4126s; Cell Signaling Technology); anti–PKA-RIα (610609;

BD Biosciences, San Jose, CA); anti–PKA-RIIβ (610625; BD Biosciences); and anti-PKAα catalytic subunit (C-20) (sc-903; Santa Cruz Biotechnology). Anti-Ubxd8 antibody was provided by the laboratory of Dr. James Olzmann (University of California, Berkeley). The intensity of the bands was quantified using ImageJ software (National Institute of Health) and normalized to GAPDH or Ubxd8 as indicated.

PDE Activity Assay

Total protein lysates were prepared from fresh tissues, and PDE activity was measured with PDELight HTS cAMP phosphodiesterase kit (LT07–600; Lonza, Anaheim, CA).

Statistics

We used a Student t test, and data were expressed as the SEM for each group. P values <0.05 were considered to be significant.

RESULTS

Dex Treatment Increased Pik3r1 Protein in WAT Depots

We have previously identified Pik3r1 as a GC primary target gene in 3T3-L1 adipocytes, and here we examined whether GCs induce Pik3r1 protein levels in vivo. Dex, a synthetic GC, was administered intraperitoneally for 1, 4, or 7 days in floxed Pik3r1 mice (33) (*Pik3r1$^{flox/flox}$*, referred to as WT) mice. Compared with PBS injection, Dex treatment increased the levels of Pik3r1 protein by as soon as 1 day by twofold in both iWAT (Fig. 1A) and eWAT (Fig. 1B). By the end of 7 days, Dex elevated Pik3r1 protein levels by approximately threefold in both adipose depots (Fig. 1A and B). These results demonstrated that GCs increase Pik3r1 protein expression in iWAT and eWAT in vivo.

To study the role of Pik3r1 in GC-promoted lipolysis, we generated adipose tissue–specific Pik3r1-null mice with AdipoQ-Cre (34) and floxed Pik3r1 mice (33) and termed AKO mice for simplicity. To confirm the knockout efficiency and tissue specificity, we isolated iWAT, eWAT, liver, and gastrocnemius (GA) muscle from 8-week-old AKO mice and control littermates. Immunoblotting shows total ablation of Pik3r1 protein in iWAT and eWAT from AKO mice, although their expressions are present in both depots from WT mice (Fig. 1C). Furthermore, Pik3r1 expression is intact in the liver and GA muscle of AKO mice (Fig. 1D). These data demonstrated extremely high efficiency and specificity for the knockout line. Importantly, AKO mice showed no gross phenotype and maintained a body weight that was similar to that of their control littermates (Fig. 1E).

Dex-Induced WAT Lipolysis Was Absent in AKO Mice

We hypothesize that Pik3r1 mediates Dex-induced lipolysis in iWAT and eWAT. We injected a single dose of Dex (10 mg/kg body wt) or control PBS in AKO and WT mice. This dose of Dex was somewhat high. However, pilot studies in our laboratory have shown that lower doses of Dex induced a weak lipolytic effect in these mice of mixed FVB/BL6/SV129 background. Higher doses of Dex provide a stronger lipolytic response and therefore allow us to dissect the mechanisms underlying Dex effects. Notably, another laboratory similarly found that mice containing the FVB background are less sensitive to GC-regulated physiological phenotypes (37). Twenty-four hours after injection, glycerol release from isolated iWAT and eWAT was measured. The amount of released glycerol indicates the degree of lipolysis. In WT mice, Dex induced glycerol release in both iWAT and eWAT explants (Fig. 2A and B). In contrast, in AKO mice, Dex-stimulated glycerol release was absent (Fig. 2A and B). Furthermore, we also measured the levels of plasma FFA, the other product of lipolysis. Plasma FFA levels were increased in Dex-treated WT mice (Fig. 2C). However, Dex failed to induce plasma FFA in AKO mice (Fig. 2C). These results illustrated that Pik3r1 is required for Dex-initiated WAT lipolysis.

Dex-Stimulated ATGL Expression Was Unaffected in AKO Mice

To understand the mechanism of impaired Dex-induced WAT lipolysis in the absence of Pik3r1, we first examined ATGL, the rate-controlling enzyme in lipolysis. Previous studies have shown that the expression of ATGL was highly induced by GCs (8,9). To examine whether Dex-increased ATGL expression was affected in the absence of Pik3r1, we treated AKO and WT mice with Dex or PBS for 24 h and performed protein and mRNA expression analysis. Consistent with previous reports (12), Dex elevated ATGL protein and mRNA levels in iWAT and eWAT of WT mice (Fig. 3A and B). Notably, the absence of Pik3r1 did not affect the ability of Dex to elevate protein and mRNA expression of ATGL (Fig. 3A and B).

Dex Induced the Phosphorylation of HSL but Not Plin1 in AKO Mice

A second mechanism in which GC-induced lipolysis is through phosphorylation of HSL and Plin1 indirectly, and we tested whether Pik3r1 was required in this process. HSL and Plin1 are phosphorylated by PKA, at serine 660 for HSL (38) and serine 517 for Plin1 (39). In iWAT and eWAT, the levels of total HSL showed an upward trend in WT and AKO mice treated with Dex but did not reach statistical significance (Fig. 4A and B). In contrast, pHSL levels were increased by Dex in iWAT and eWAT from WT and AKO mice (Fig. 4C). These data showed that a lack of Pik3r1 did not affect Dex-increased pHSL levels.

In both adipose depots, the levels of total Plin1 displayed similar levels in WT and AKO mice treated with Dex (Fig. 4D and E). Dex increased pPlin1 in WT mice but failed to do so in AKO mice (Fig. 4F). Thus, Pik3r1 is essential for Dex to induce phosphorylation of Plin1.

Pik3r1 Is Dispensable in Dex-Modulated Akt and PDE Activities

Insulin suppresses WAT lipolysis in part through a PI3K-Akt-PDE3B pathway, where the secondary messenger cAMP is degraded and therefore unable to activate PKA. In the iWAT depot, total Akt protein levels were decreased by Dex
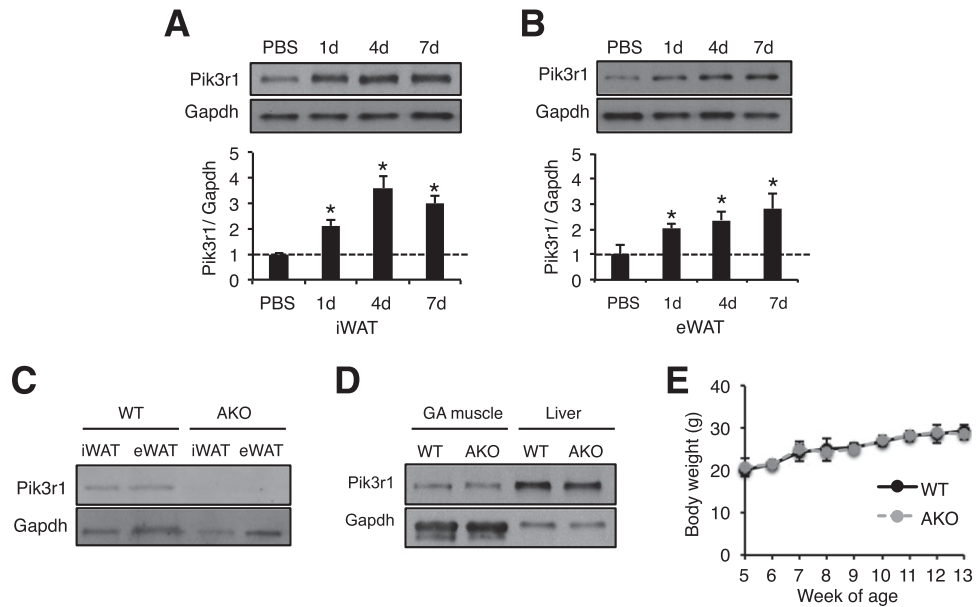
Figure 1—Dex induced Pik3r1 protein expression in iWAT and eWAT. A and B: Eight-week-old male WT mice were injected intraperitoneally with control PBS or Dex (water-soluble Dex, 5 mg/kg body wt; D2915; Sigma-Aldrich) for 1, 4, or 7 days. Pik3r1 protein expression was measured with immunoblotting in iWAT (A) and eWAT (B) and was normalized to internal control GAPDH. Representative immunoblots are shown (n = 3). Error bars represent the SEM of relative Pik3r1 expression level (Dex vs. PBS). *$P < 0.05$. In 8-week-old male WT and AKO mice, Pik3r1 expressions were examined in iWAT and eWAT (C) and in GA muscle and liver (D). E: Body weights of WT and AKO mice were monitored from age 5 to 13 weeks; n = 6. Error bars represent the SEM.

in WT mice but were upregulated by Dex in AKO mice (Fig. 5A and B). In contrast, no difference was observed in the eWAT depot (Fig. 5A and B). This suggests that GCs exert a depot-specific effect on total Akt protein expression.

For Akt activity, we monitored the phosphorylation status of Akt at serine 308 (40). In both iWAT and eWAT, Dex-induced phosphorylation of Akt displayed the same trend in WT and AKO mice (Fig. 5A and C). Dex did not affect the levels of FoxO1, a downstream effector of Akt. However, the effects of Dex on the phosphorylation status of FoxO1 (phosphorylated FoxO1/FoxO1) were

similar to those of Akt (Supplementary Fig. 1). These results demonstrated that the effects of Dex on PI3K-Akt signaling were not affected in Pik3r1-null mice, likely due to the redundant function of Pik3r2.

We further examined PDE activities. Compared with control-treated WT mice, control-treated AKO mice and Dex-treated WT and AKO mice all showed increased PDE activities in iWAT (Fig. 5D). In eWAT, only Dex-treated WT mice showed significant PDE activity induction. Although the elevation of control- and Dex-treated eWAT in AKO mice did not reach statistical significance, the upward trend
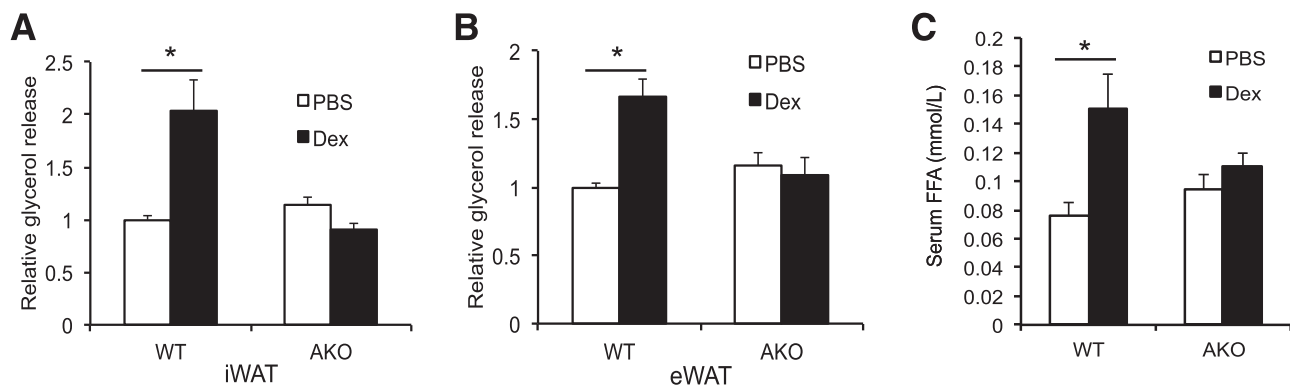

Figure 2—Dex-stimulated WAT lipolysis was abolished in AKO mice. Eight-week-old male WT and AKO mice were administered PBS or Dex (10 mg/kg body wt) at 10:00 A.M. in the morning. After 24 h (at 10:00 A.M. the next morning), fat pads of iWAT and eWAT were isolated for lipolysis assays. Relative glycerol release was measured from iWAT (A) and eWAT (B) explants. C: The levels of serum FFAs were measured. Error bars represent the SEM. n = 7. *$P < 0.05$.
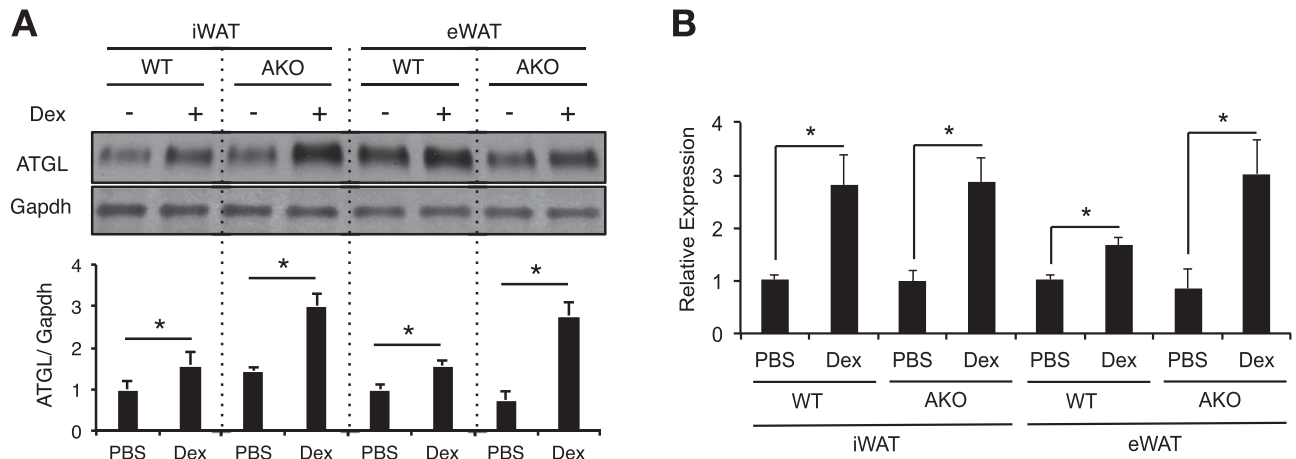
Figure 3—Dex increased ATGL protein and mRNA expression in WT and AKO mice. Eight-week-old male WT and AKO mice were administered PBS or Dex (10 mg/kg body wt) for 24 h. A: In both iWAT and eWAT, the expression of ATGL was monitored by immunoblots. Representative results from three independent experiments are shown. Bar graphs show the average intensity of bands. GAPDH was used as an internal control. B: The mRNA expression level of ATGL was monitored by quantitative real-time PCR. Error bars represent the SEM. *$P < 0.05$.

demonstrated that their PDE signaling was unchanged (Fig. 5D).

It was surprising that Dex treatment increased Akt and PDE activities (Fig. 5C and D), since GCs have been shown to antagonize insulin signaling in adipocytes (20,41–43). Moreover, GC-induced excess Pik3r1 did not inhibit Akt and PDE activities. Notably, the treatment of GCs in vivo causes hyperinsulinemia, which could explain the elevated
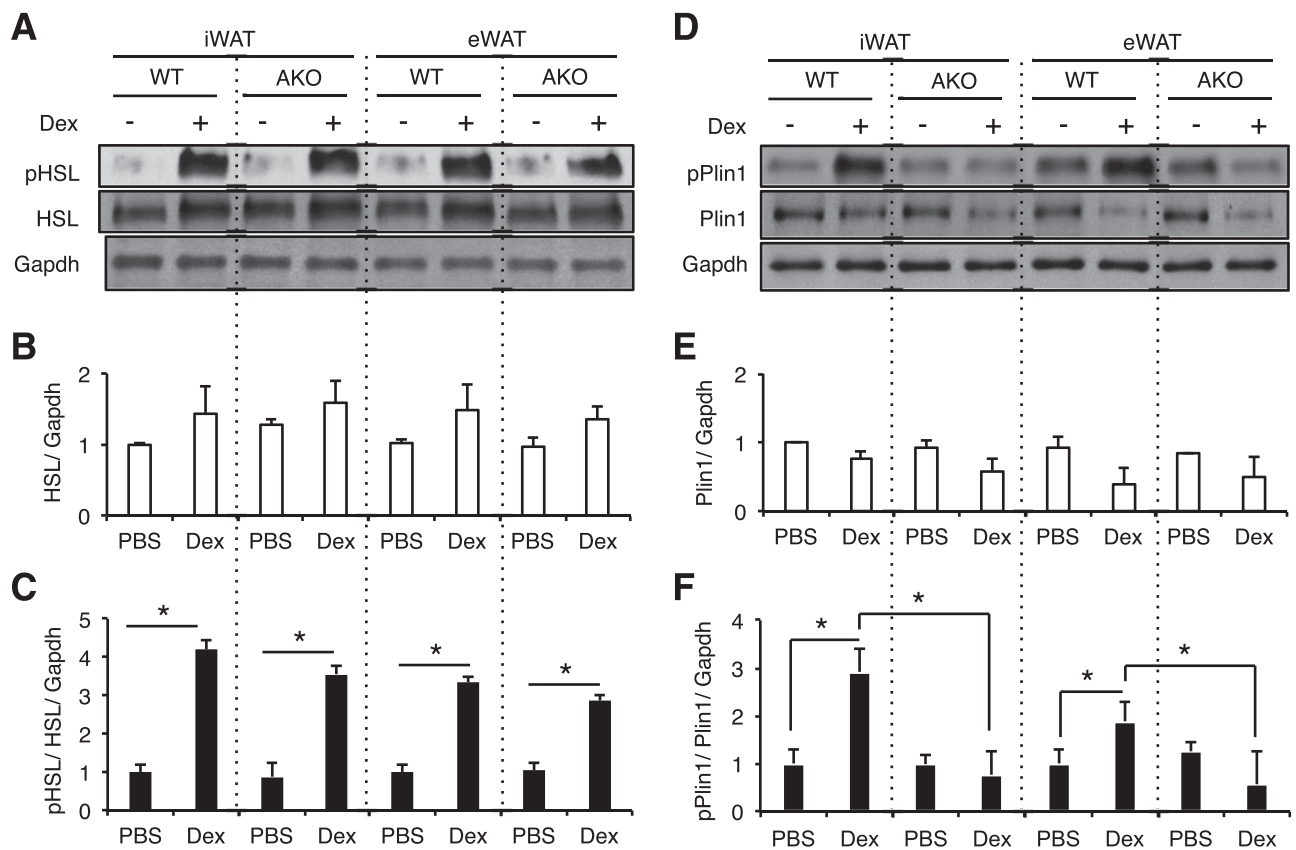

Figure 4—Dex effects on HSL and Plin1 phosphorylation in WT and AKO mice. Eight-week-old male WT and AKO mice were administered PBS or Dex (10 mg/kg body wt) for 24 h. A: In iWAT and eWAT, HSL and pHSL levels are displayed in immunoblots, and GAPDH was used as an internal control. B: Bar graphs show normalized total HSL protein levels. C: Bar graphs illustrate normalized pHSL protein levels. D: In iWAT and eWAT, Plin1 and pPlin1 levels are displayed in immunoblots, and GAPDH was used as an internal control. E: Bar graphs show normalized total Plin1 protein levels. F: Bar graphs illustrate normalized pPlin1 protein levels. Error bars represent the SEM. $n = 3$. *$P < 0.05$.
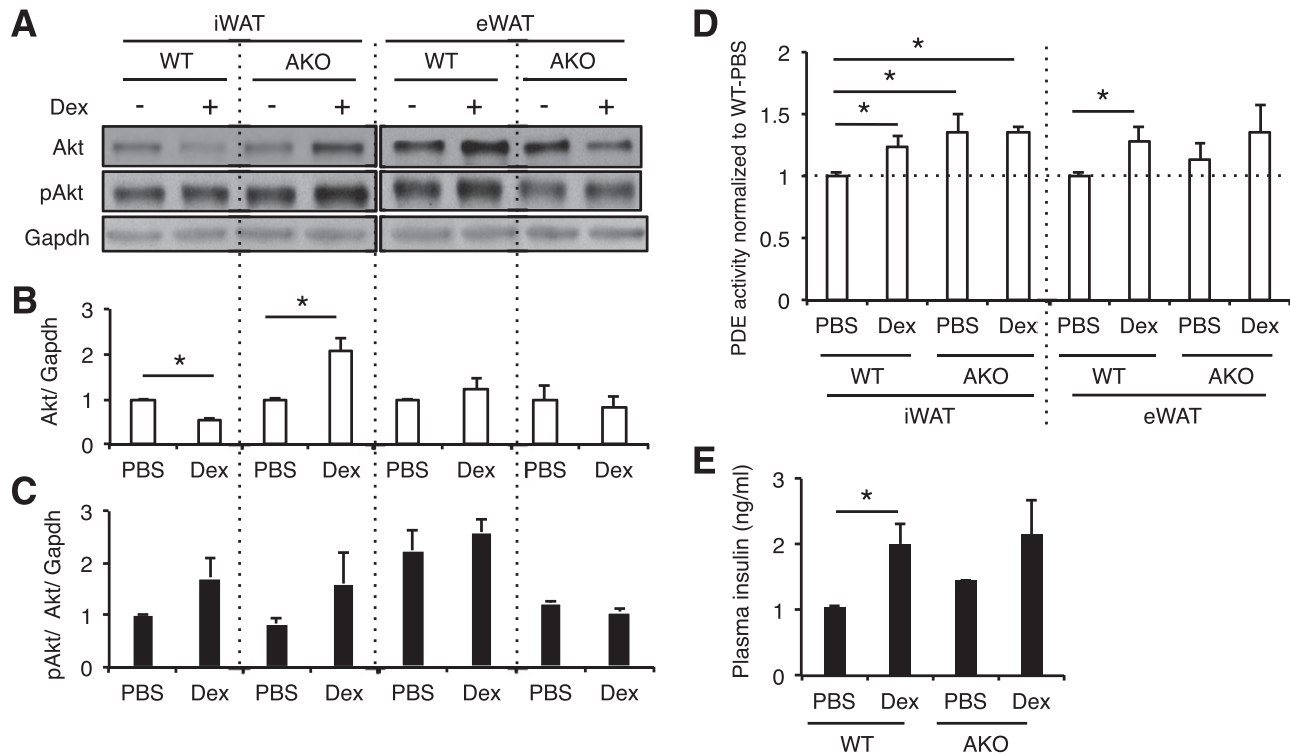
Figure 5—Dex actions on Akt and PDE activities are intact in the absence of Pik3r1. Eight-week-old male WT and AKO mice were administered PBS or Dex (10 mg/kg body wt) for 24 h. A: In iWAT and eWAT, Akt and pAkt levels are displayed in immunoblots, and GAPDH was used as an internal control. B: Bar graphs show normalized total Akt protein levels. C: Bar graphs illustrate normalized pAkt protein levels. D: In iWAT and eWAT, PDE activities are normalized to PBS-treated WT mice. E: Plasma insulin levels were measured. Error bars represent the SEM. $n = 6$. *$P < 0.05$.

Akt and PDE activities. To examine this, we measured the plasma insulin levels in Dex-treated WT and AKO mice. Indeed, we found that Dex increased insulin levels in WT mice, and a similar upward trend was observed in AKO mice (Fig. 5E). These data demonstrated that the PI3K-Akt-PDE3B pathway was intact even in the absence of Pik3r1. Thus, Dex-induced PKA signaling was independent of the PI3K-Akt-PDE3B pathway.

In the Lipid Droplets, Dex Increased pHSL and Subunits of PKA Were Attenuated in AKO Mice

We further explored the mechanism of compromised Dex-induced Plin1 phosphorylation in the absence of Pik3r1 in the lipid droplet and proposed three scenarios. First, the amount of PKA in the lipid droplet could be reduced. Second, the levels of the lipid droplet A kinase–anchoring protein optic atrophy 1 (OPA1) (44) could decrease. This results in less anchored PKA in lipid droplets. Third, pPlin1 could be dephosphorylated more rapidly. We isolated lipid droplets from eWAT from control- or Dex-treated WT and AKO mice and tested these possibilities.

Pik3r1 is present in lipid droplets in WT mice but not in AKO mice. Interestingly, Dex did not modulate Pik3r1 protein levels in these lipid droplets (Fig. 6A). In contrast, Dex increased the phosphorylation of lipid droplet–associated HSL and Plin1 in WT mice but not in AKO

mice (Fig. 6A–C). Furthermore, Dex increased the levels of PKA catalytic and regulatory RIIβ subunit in lipid droplets of WT mice but not AKO mice (Fig. 6A, D, and E). OPA1, however, showed no difference between WT and AKO mice. Protein phosphatase 1 (PP1) dephosphorylates lipid droplet–anchored Plin1 (45), and similar levels of PP1 were detected in WT and AKO mice (Fig. 6A). To test whether Dex generally increases PKA levels, we monitored different subunits of PKA in whole-cell lysates of eWAT from WT and AKO mice treated with Dex, and no difference was found (Supplementary Fig. 2). Overall, these results indicate that Pik3r1 is indispensable for Dex-increased pPlin1, pHSL, and PKA levels in lipid droplets.

AKO Mice Were Protected From Dex-Induced Hepatic Steatosis and Hypertriglyceridemia

Superfluous adipose tissue lipolysis caused by GCs can result in excess lipid mobilization from WAT to liver, leading to hepatic steatosis and hypertriglyceridemia. We explored the possibility that Pik3r1 ablation could relieve GC-induced symptoms. Dex was administered to WT and AKO mice for 7 days, and their plasma and hepatic TG levels were measured. Similar levels of hepatic TGs were found in control-treated WT and AKO mice (Fig. 7A). Dex stimulated hepatic TG levels by 10-fold in WT mice (Fig. 7A). Markedly, this adverse Dex effect was reduced to only
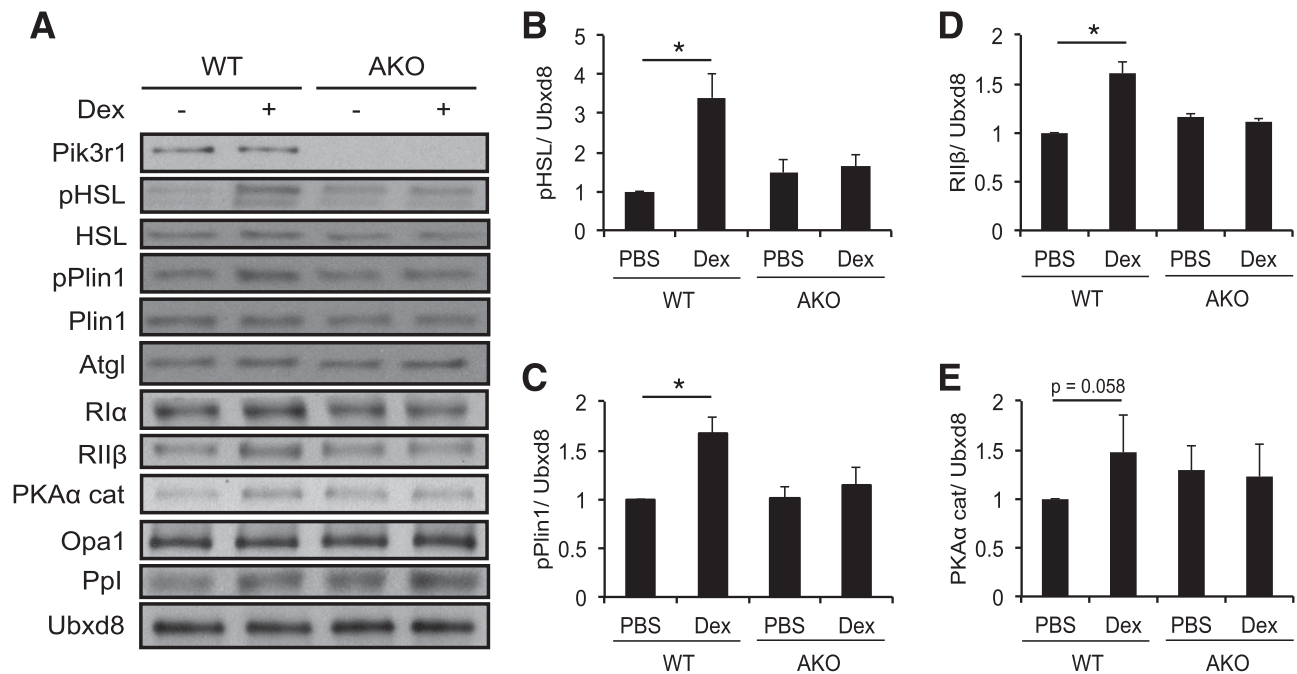
Figure 6—In lipid droplets, Dex induced the levels of pHSL, pPlin1, and subunits of PKA in WAT of WT mice but not AKO mice. Eight-week-old male WT and AKO mice were administered PBS or Dex (10 mg/kg body wt) for 24 h. A–E: Lipid droplets were isolated from eWAT. A: Immunoblots display the levels of Pik3r1, pHSL, pPlin1, regulatory subunits of PKA (PKA-RIα and PKA-RIIβ), catalytic subunit of PKA (PKAα-cat), OPA1, PP1, and lipid droplet internal control Ubxd8. B: Bar graphs show normalized pHSL protein levels. C: Bar graphs show normalized pPlin1 protein levels. D: Bar graphs illustrate normalized PKA-RIIβ protein levels. E: Bar graphs demonstrate normalized PKAα-cat protein levels. Error bars represent the SEM. $n = 3$. *$P < 0.05$.

twofold in AKO mice (Fig. 7A). For plasma TG, levels were similar between control-treated WT and AKO mice (Fig. 7B). In WT mice, Dex increased plasma TG levels by twofold (Fig. 7B). However, this effect was abolished in AKO mice (Fig. 7B). These results demonstrated that Pik3r1 ablation improves GC-induced hepatic steatosis and hypertriglyceridemia.

We performed an intraperitoneal glucose tolerance test in control- and Dex-treated WT and AKO mice. We found that glucose tolerance was similar between control- and Dex-treated WT and AKO mice (Supplementary Fig. 3A and B). Plasma insulin levels were lower in control-treated AKO mice than in WT mice (Supplementary Fig. 3C). In both WT and AKO mice, Dex treatment caused hyperinsulinemia (Supplementary Fig. 3C). However, plasma insulin levels for Dex-treated AKO mice were significantly lower than those of Dex-treated WT mice (Supplementary Fig. 3C). These results suggest that Dex-treated AKO mice were more insulin sensitive than Dex-treated WT mice.

Norepinephrine-Increased WAT Lipolysis Was Not Affected in AKO Mice

In addition to GCs, norepinephrine plays a key role in promoting WAT lipolysis (11). WT and AKO mice were treated with or without norepinephrine for 20 min. Plasma FFA levels were then measured. Norepinephrine treatment significantly increased the levels of plasma FFA in both WT and AKO mice. The fold induction of norepinephrine was

similar, although plasma FFA levels were slightly lower in AKO mice (Supplementary Fig. 4A). We isolated eWAT from WT and AKO mice to perform ex vivo lipolysis assay. We found that norepinephrine significantly elevated glycerol release from eWAT explants of WT and AKO mice (Supplementary Fig. 4B). The fold induction of norepinephrine was similar between WT and AKO eWAT explants (Supplementary Fig. 4B). These results demonstrate that norepinephrine-induced adipocyte lipolysis is not affected by lacking Pik3r1.

DISCUSSION

Endogenous GCs are essential for metabolic adaptation in stressful conditions such as fasting. During fasting, GCs promote lipolysis in adipose tissues to release glycerol for hepatic gluconeogenesis and fatty acids as energy fuels for peripheral tissues. However, during prolonged GC exposure, such as in exogenous anti-inflammation treatment, excess lipolysis can cause metabolic disorders, including dyslipidemia and insulin resistance. Therefore, identification of GC targets in adipose tissue is critical to eliminate the adverse metabolic actions in GC therapeutic agents. Here, we report that Pik3r1, a regulatory subunit of PI3K and a GC primary target gene, mediates GC-stimulated adipocyte lipolysis. With the deletion of Pik3r1 in WAT specifically, the ability of GCs to induce lipolysis was abolished, and GC-initiated hepatic steatosis and hypertriglyceridemia
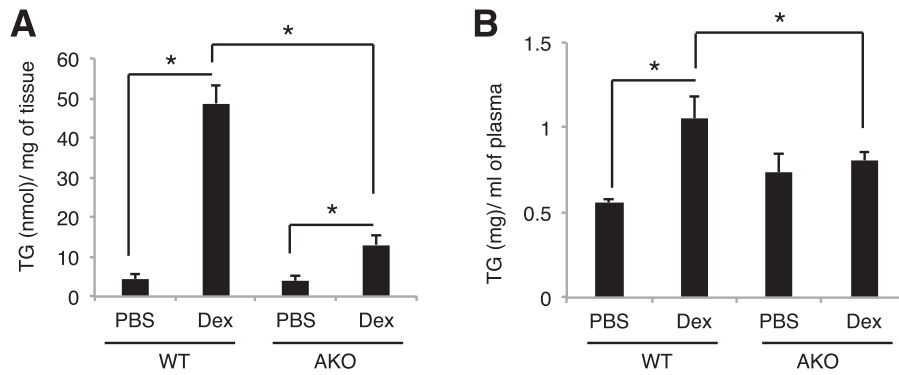
Figure 7—AKO mice are protected from Dex-induced hepatic steatosis and hypertriglyceridemia. Eight-week-old male WT and AKO mice were administered PBS or Dex (10 mg/kg body wt) for 7 days. Hepatic TG (A) and plasma TG (B) levels were assessed. For plasma TGs, mice were fasted for 6 h prior to sample collection. Error bars represent the SEM. $n = 6$. *$P < 0.05$.

were alleviated. We then explored the potential mechanisms of reduced GC-stimulated lipolysis in the absence of Pik3r1.

Because Pik3r1 participates in PI3K-Akt-PDE3B axis, Pik3r1 deletion could impair this axis therefore antagonizing cAMP-PKA–induced lipolysis. Unexpectedly, this axis was very much intact in Pik3r1-null adipocytes upon 24 h of Dex treatment. Thus, Pik3r1 is involved in GC-promoted WAT lipolysis through a pathway independent of the PI3K-Akt axis. Interestingly, although similar levels of pHSL were found in whole-cell lysates in the WAT of WT and AKO mice in response to GC treatment, its levels in lipid droplets of WAT in AKO mice were markedly reduced. This is likely due to the reduced pPlin1 levels in WAT of Dex-treated AKO mice because the PKA phosphorylation of Plin1 is required for its recruitment of pHSL to the lipid droplet (46,47). Notably, subunits of PKA in lipid droplets were increased by GC treatment in WT mice but not AKO mice, whereas their levels in whole-cell lysates were similar in both mouse models. On the basis of these results, we propose that without Pik3r1 in adipocytes, the ability of Dex to increase PKA levels in the lipid droplet is impaired, resulting in reduced pPlin1 levels in the lipid droplet (Fig. 8). As a result, the levels of GC-induced pHSL levels were eradicated in the lipid droplet, which caused the impairment of lipolysis (Fig. 8). Thus, Pik3r1 plays a role in recruiting PKA to the lipid droplet in conveying GC-induced adipocyte lipolysis. Notably, upon a prolonged Dex exposure it is possible that the role of Pik3r1 in the regulation of insulin sensitivity is involved in the modulation of WAT lipolysis. This speculation is based on the fact that AKO mice were more insulin sensitive than WT mice upon 7 days of Dex treatment. Moreover, the improvement of insulin sensitivity could also contribute to improved hepatic steatosis and hypertriglyceridemia phenotypes in Dex-treated AKO mice.
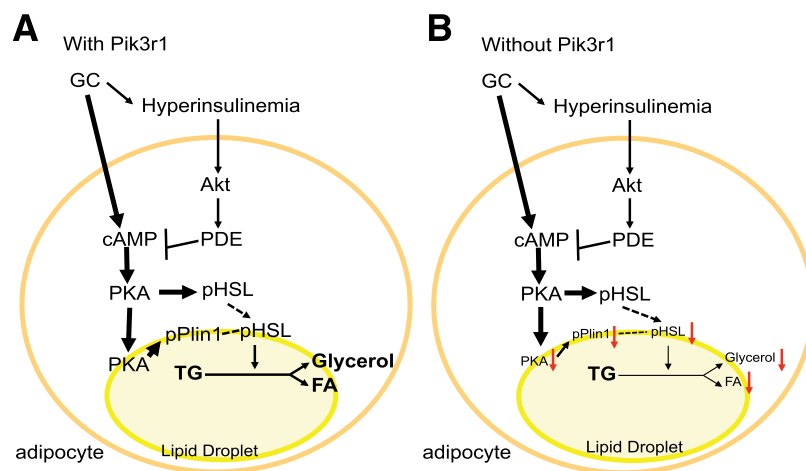

Figure 8—A model for the role of Pik3r1 in GC-stimulated WAT lipolysis. In WAT, PI3K-Akt-PDE3B signaling was intact in the absence of Pik3r1 (in gray). A: In the presence of Pik3r1, GC treatment augments cAMP-PKA signaling, leading to the phosphorylation of HSL in the cytosol. In the lipid droplets, PKA levels, which in turn phosphorylate Plin1, are increased. pPlin1 can then anchor pHSL from the cytosol to lipid droplets for TG hydrolysis. B: In the absence of Pik3r1, GC-induced cAMP-PKA signaling is still able to phosphorylate cytosolic HSL. However, GCs did not increase PKA levels in the lipid droplet. Plin1 cannot be phosphorylated, and pHSL is unable to anchor to the lipid droplet; therefore, minimal lipolysis was observed. Red arrows indicate the reduction of levels in lipid droplet. FA, fatty acid.

So, how is Pik3r1 involved in GC-increased PKA levels in the lipid droplet? OPA1 plays a key role in anchoring PKA in the lipid droplet to phosphorylate Plin1 upon catecholamine stimulation (44). However, our studies showed that GC treatment did not affect the levels of OPA1 in the lipid droplet. We cannot exclude the possibility that GCs induce post-translational modifications of OPA1 to increase the retention of PKA in the lipid droplet. Alternatively, GCs could increase the trafficking of PKA to the lipid droplet. Pik3r1 has been shown to participate in the trafficking of receptor tyrosine kinases and erythropoietin receptor (48,49) and is required for the nuclear localization of XBP1 (50,51). Another possibility is that Pik3r1 is involved in PKA stability in the lipid droplet. Pik3r1 has been shown to interact with PTEN and blocks ubiquitination of PTEN and its eventual proteasomal degradation (52). Future experiments are necessary to determine which of these mechanisms are exerted by Pik3r1 to increase PKA levels in the lipid droplet upon GC treatment.

We have previously shown that *Angptl4*, another GR primary target gene (21), is involved in GC-induced adipocyte lipolysis. *Angptl4* encodes a secreted protein that directly increases cAMP levels in adipocytes to promote lipolysis. In *Angptl4*-null mice, PKA-initiated phosphorylation of HSL and Plin1 induced by Dex are significantly reduced (12). Thus, Angptl4 acts upstream of Pik3r1 in GC-induced adipose lipolysis. In this view, it would be interesting to examine whether Angptl4-induced adipose lipolysis requires Pik3r1.

Notably, norepinephrine also activates cAMP-PKA signaling to stimulate lipolysis. However, Pik3r1 is not required for norepinephrine-induced adipocyte lipolysis. In contrast to GCs, norepinephrine does not increase Pik3r1 expression in adipocytes. We speculate that in normal physiological states, the majority of Pik3r1 is associated with the catalytic subunit of PI3K. GCs increase the levels of Pik3r1, which in turn can participate in lipolysis in adipocytes. This model will need to be examined in a future study.

In summary, our studies have identified a novel role of Pik3r1 in GC-augmented PKA levels in the lipid droplet to promote lipolysis. Removal of Pik3r1 in WAT dampens the ability of GCs to promote lipolysis, which leads to hypertriglyceridemia and fatty liver. Thus, WAT Pik3r1 is a potential target to lessen lipid disorders caused by GCs. The mechanisms underlying the regulation of PKA levels in the lipid droplet that leads to the modulation of lipolysis is mostly unknown, and future studies are warranted.

References

1. Kuo T, McQueen A, Chen TC, Wang JC. Regulation of glucose homeostasis by glucocorticoids. Adv Exp Med Biol 2015;872:99–126

2. de Guia RM, Herzig S. How do glucocorticoids regulate lipid metabolism? Adv Exp Med Biol 2015;872:127–144

3. Macfarlane DP, Forbes S, Walker BR. Glucocorticoids and fatty acid metabolism in humans: fuelling fat redistribution in the metabolic syndrome. J Endocrinol 2008;197:189–204

4. Rhen T, Cidlowski JA. Antiinflammatory action of glucocorticoids—new mechanisms for old drugs. N Engl J Med 2005;353:1711–1723

5. Campbell JE, Peckett AJ, D'souza AM, Hawke TJ, Riddell MC. Adipogenic and lipolytic effects of chronic glucocorticoid exposure. Am J Physiol Cell Physiol 2011;300:C198–C209

6. Peckett AJ, Wright DC, Riddell MC. The effects of glucocorticoids on adipose tissue lipid metabolism. Metabolism 2011;60:1500–1510

7. Fain JN, Dodd A, Novak L. Enzyme regulation in gluconeogenesis and lipogenesis. Relationship of protein synthesis and cyclic AMP to lipolytic action of growth hormone and glucocorticoids. Metabolism 1971;20:109–118

8. Yu CY, Mayba O, Lee JV, et al. Genome-wide analysis of glucocorticoid receptor binding regions in adipocytes reveal gene network involved in triglyceride homeostasis. PLoS One 2010;5:e15188

9. Villena JA, Roy S, Sarkadi-Nagy E, Kim KH, Sul HS. Desnutrin, an adipocyte gene encoding a novel patatin domain-containing protein, is induced by fasting and glucocorticoids: ectopic expression of desnutrin increases triglyceride hydrolysis. J Biol Chem 2004;279:47066–47075

10. Young SG, Zechner R. Biochemistry and pathophysiology of intravascular and intracellular lipolysis. Genes Dev 2013;27:459–484

11. Duncan RE, Ahmadian M, Jaworski K, Sarkadi-Nagy E, Sul HS. Regulation of lipolysis in adipocytes. Annu Rev Nutr 2007;27:79–101

12. Gray NE, Lam LN, Yang K, Zhou AY, Koliwad S, Wang JC. Angiopoietin-like 4 (Angptl4) protein is a physiological mediator of intracellular lipolysis in murine adipocytes. J Biol Chem 2012;287:8444–8456

13. Koliwad SK, Gray NE, Wang JC. Angiopoietin-like 4 (Angptl4): a glucocorticoid-dependent gatekeeper of fatty acid flux during fasting. Adipocyte 2012;1:182–187

14. Xu C, He J, Jiang H, et al. Direct effect of glucocorticoids on lipolysis in adipocytes. Mol Endocrinol 2009;23:1161–1170

15. Moore HP, Silver RB, Mottillo EP, Bernlohr DA, Granneman JG. Perilipin targets a novel pool of lipid droplets for lipolytic attack by hormone-sensitive lipase. J Biol Chem 2005;280:43109–43120

16. Brasaemle DL, Subramanian V, Garcia A, Marcinkiewicz A, Rothenberg A. Perilipin A and the control of triacylglycerol metabolism. Mol Cell Biochem 2009; 326:15–21

17. Sztalryd C, Kimmel AR. Perilipins: lipid droplet coat proteins adapted for tissue-specific energy storage and utilization, and lipid cytoprotection. Biochimie 2014;96:96–101

18. Subramanian V, Rothenberg A, Gomez C, et al. Perilipin A mediates the reversible binding of CGI-58 to lipid droplets in 3T3-L1 adipocytes. J Biol Chem 2004;279:42062–42071

19. Granneman JG, Moore HP, Krishnamoorthy R, Rathod M. Perilipin controls lipolysis by regulating the interactions of AB-hydrolase containing

5 (Abhd5) and adipose triglyceride lipase (Atgl). J Biol Chem 2009;284:34538–34544

20. Burén J, Lai YC, Lundgren M, Eriksson JW, Jensen J. Insulin action and signalling in fat and muscle from dexamethasone-treated rats. Arch Biochem Biophys 2008;474:91–101

21. Koliwad SK, Kuo T, Shipp LE, et al. Angiopoietin-like 4 (ANGPTL4, fasting-induced adipose factor) is a direct glucocorticoid receptor target and participates in glucocorticoid-regulated triglyceride metabolism. J Biol Chem 2009;284:25593–25601

22. Kuo T, Lew MJ, Mayba O, Harris CA, Speed TP, Wang JC. Genome-wide analysis of glucocorticoid receptor-binding sites in myotubes identifies gene networks modulating insulin signaling. Proc Natl Acad Sci U S A 2012;109:11160–11165

23. Barbour LA, Mizanoor Rahman S, Gurevich I, et al. Increased P85alpha is a potent negative regulator of skeletal muscle insulin signaling and induces in vivo insulin resistance associated with growth hormone excess. J Biol Chem 2005;280:37489–37494

24. Draznin B. Molecular mechanisms of insulin resistance: serine phosphorylation of insulin receptor substrate-1 and increased expression of p85alpha: the two sides of a coin. Diabetes 2006;55:2392–2397

25. Taniguchi CM, Aleman JO, Ueki K, et al. The p85alpha regulatory subunit of phosphoinositide 3-kinase potentiates c-Jun N-terminal kinase-mediated insulin resistance. Mol Cell Biol 2007;27:2830–2840

26. Luo J, Field SJ, Lee JY, Engelman JA, Cantley LC. The p85 regulatory subunit of phosphoinositide 3-kinase down-regulates IRS-1 signaling via the formation of a sequestration complex. J Cell Biol 2005;170:455–464

27. Ueki K, Fruman DA, Brachmann SM, Tseng YH, Cantley LC, Kahn CR. Molecular balance between the regulatory and catalytic subunits of phosphoinositide 3-kinase regulates cell signaling and survival. Mol Cell Biol 2002;22:965–977

28. Cheung LW, Walkiewicz KW, Besong TM, et al. Regulation of the PI3K pathway through a p85α monomer-homodimer equilibrium. eLife 2015;4:e06866

29. Chagpar RB, Links PH, Pastor MC, et al. Direct positive regulation of PTEN by the p85 subunit of phosphatidylinositol 3-kinase. Proc Natl Acad Sci U S A 2010;107:5471–5476

30. Degerman E, Ahmad F, Chung YW, et al. From PDE3B to the regulation of energy homeostasis. Curr Opin Pharmacol 2011;11:676–682

31. Degerman E, Landström TR, Wijkander J, et al. Phosphorylation and activation of hormone-sensitive adipocyte phosphodiesterase type 3B. Methods 1998;14:43–53

32. Kitamura T, Kitamura Y, Kuroda S, et al. Insulin-induced phosphorylation and activation of cyclic nucleotide phosphodiesterase 3B by the serine-threonine kinase Akt. Mol Cell Biol 1999;19:6286–6296

33. Luo J, McMullen JR, Sobkiw CL, et al. Class IA phosphoinositide 3-kinase regulates heart size and physiological cardiac hypertrophy. Mol Cell Biol 2005;25:9491–9502

34. Eguchi J, Wang X, Yu S, et al. Transcriptional control of adipose lipid handling by IRF4. Cell Metab 2011;13:249–259

35. Kuo T, Liu PH, Chen TC, et al. Transcriptional regulation of FoxO3 gene by glucocorticoids in murine myotubes. Am J Physiol Endocrinol Metab 2016;310:E572–E585

36. Blouin CM, Le Lay S, Eberl A, et al. Lipid droplet analysis in caveolin-deficient adipocytes: alterations in surface phospholipid composition and maturation defects. J Lipid Res 2010;51:945–956

37. Watson ML, Baehr LM, Reichardt HM, Tuckermann JP, Bodine SC, Furlow JD. A cell-autonomous role for the glucocorticoid receptor in skeletal muscle atrophy induced by systemic glucocorticoid exposure. Am J Physiol Endocrinol Metab 2012;302:E1210–E1220

38. Su CL, Sztalryd C, Contreras JA, Holm C, Kimmel AR, Londos C. Mutational analysis of the hormone-sensitive lipase translocation reaction in adipocytes. J Biol Chem 2003;278:43615–43619

39. Zhang HH, Souza SC, Muliro KV, Kraemer FB, Obin MS, Greenberg AS. Lipase-selective functional domains of perilipin A differentially regulate constitutive and protein kinase A-stimulated lipolysis. J Biol Chem 2003;278:51535–51542

40. Alessi DR, Andjelkovic M, Caudwell B, et al. Mechanism of activation of protein kinase B by insulin and IGF-1. EMBO J 1996;15:6541–6551

41. Houstis N, Rosen ED, Lander ES. Reactive oxygen species have a causal role in multiple forms of insulin resistance. Nature 2006;440:944–948

42. Burén J, Liu HX, Jensen J, Eriksson JW. Dexamethasone impairs insulin signalling and glucose transport by depletion of insulin receptor substrate-1, phosphatidylinositol 3-kinase and protein kinase B in primary cultured rat adipocytes. Eur J Endocrinol 2002;146:419–429

43. Wang Y, Yan C, Liu L, et al. 11β-Hydroxysteroid dehydrogenase type 1 shRNA ameliorates glucocorticoid-induced insulin resistance and lipolysis in mouse abdominal adipose tissue. Am J Physiol Endocrinol Metab 2015;308:E84–E95

44. Pidoux G, Witczak O, Jarnæss E, et al. Optic atrophy 1 is an A-kinase anchoring protein on lipid droplets that mediates adrenergic control of lipolysis. EMBO J 2011;30:4371–4386

45. Clifford GM, McCormick DK, Londos C, Vernon RG, Yeaman SJ. Dephosphorylation of perilipin by protein phosphatases present in rat adipocytes. FEBS Lett 1998;435:125–129

46. Sztalryd C, Xu G, Dorward H, et al. Perilipin A is essential for the translocation of hormone-sensitive lipase during lipolytic activation. J Cell Biol 2003;161:1093–1103

47. Wang H, Hu L, Dalen K, et al. Activation of hormone-sensitive lipase requires two steps, protein phosphorylation and binding to the PAT-1 domain of lipid droplet coat proteins. J Biol Chem 2009;284:32116–32125

48. Chamberlain MD, Berry TR, Pastor MC, Anderson DH. The p85alpha subunit of phosphatidylinositol 3′-kinase binds to and stimulates the GTPase activity of Rab proteins. J Biol Chem 2004;279:48607–48614

49. Bulut GB, Sulahian R, Yao H, Huang LJ. Cbl ubiquitination of p85 is essential for Epo-induced EpoR endocytosis. Blood 2013;122:3964–3972

50. Park SW, Zhou Y, Lee J, et al. The regulatory subunits of PI3K, p85alpha and p85beta, interact with XBP-1 and increase its nuclear translocation. Nat Med 2010;16:429–437

51. Winnay JN, Boucher J, Mori MA, Ueki K, Kahn CR. A regulatory subunit of phosphoinositide 3-kinase increases the nuclear accumulation of X-box-binding protein-1 to modulate the unfolded protein response. Nat Med 2010;16:438–445

52. Cheung LW, Hennessy BT, Li J, et al. High frequency of PIK3R1 and PIK3R2 mutations in endometrial cancer elucidates a novel mechanism for regulation of PTEN protein stability. Cancer Discov 2011;1:170–185